JOURNAL OF VIROLOGY, Sept. 2004, p. 9790–9797 Vol. 78, No. 18
0022-538X/04/$08.00+0 DOI: 10.1128/JVI.78.18.9790–9797.2004

Integral Membrane Protein P16 of Bacteriophage PRD1 Stabilizes the Adsorption Vertex Structure

Silja T. Jaatinen, Salla J. Viitanen, Dennis H. Bamford, and Jaana K. H. Bamford*

Faculty of Biosciences and Institute of Biotechnology, Viikki Biocenter, University of Helsinki, Helsinki, Finland

Received 13 February 2004/Accepted 26 April 2004

The icosahedral membrane-containing double-stranded DNA bacteriophage PRD1 has a labile receptor binding spike complex at the vertices. This complex, which is analogous to that of adenovirus, is formed of the penton protein P31, the spike protein P5, and the receptor binding protein P2. Upon infection, the internal phage membrane transforms into a tubular structure that protrudes through a vertex and penetrates the cell envelope for DNA injection. We describe here a new class of PRD1 mutants lacking virion-associated integral membrane protein P16. P16 links the spike complex to the viral membrane and is necessary for spike stability. We also show that the unique vertex used for DNA packaging is intact in the P16-deficient particle, indicating that the 11 adsorption vertices and the 1 portal vertex are functionally and structurally distinct.

PRD1 is the type organism of the *Tectiviridae* family (4, 5, 31). It is a broad-host-range bacterial virus that infects a variety of gram-negative hosts harboring an N, P, or W incompatibility group conjugative antibiotic resistance plasmid (46). The plasmid encodes a type IV transenvelope DNA translocation complex, which functions as a receptor for PRD1. The PRD1 virion consists of an icosahedral protein capsid surrounding an internal membrane that encloses the 14,927-bp linear double-stranded DNA (dsDNA) genome (see Fig. 1). The genome has 110-bp inverted terminal repeat sequences and 5′ covalently linked terminal proteins at both ends. It is replicated by a protein priming, sliding-back mechanism similar to that described for phage ϕ29 and adenovirus genomes (52).

Cryoelectron microscopy-based image reconstruction revealed that the icosahedral, tailless PRD1 has an outer diameter of 740 Å between opposite vertices (22, 54). The trimeric protein capsid is organized on a pseudo-$T = 25$ lattice with 240 copies of the coat protein trimers, like the adenovirus capsid (22). Furthermore, the structure of the trimeric PRD1 capsid protein P3 was determined to 1.65 Å resolution by X-ray crystallography, showing that the fold (two viral eight-stranded jelly rolls forming a pseudohexagonal architecture) very closely resembles that of the adenovirus coat protein, the hexon (14, 15, 16). The viral jelly roll is a common structural motif (33, 48), but the double-barrel trimer has thus far been found only in adenovirus, PRD1, and *Paramecium bursaria Chlorella* virus 1 (PBCV-1), which belongs to the family *Phycodnaviridae* (42, 60). PBCV-1 is a very large dsDNA virus with 1,680 trimeric Vp54 coat proteins arranged on a pseudo-$T = 169$ lattice (68) and a linear dsDNA genome with covalently closed hairpin ends (61, 62). Like PRD1, it contains a membrane beneath its icosahedral protein coat (56, 61, 68) and a special vertex (61). The discovery of the common trimeric double-barrel capsomer has led to the hypothesis that *Tectiviridae*, *Adenoviridae*, *Phycodnaviridae*, and most probably some other viral families (such as *Iridoviridae* and *Asfarviridae*) form a lineage with an early common ancestor (6, 7, 42). One representative of this lineage is *Bacillus thuringiensis* phage *Bam35*, a member of the *Tectiviridae* family that infects gram-positive bacteria (1, 5). Despite having no sequence similarity to PRD1, it seems to have a similar genome size and organization (47), and its coat protein sequence can be threaded onto the X-ray structure of PRD1 coat protein (S. D. Benson, J. K. H. Bamford, D. H. Bamford., and R. M. Burnett, submitted for publication).

The 66-MDa PRD1 virion with the inner membrane and DNA has been crystallized (12). The atomic resolution structure revealed the icosahedrally ordered elements of the virion, including the viral membrane (J. J. B. Cockburn, N. G. A. Abrescia, J. M. Grimes, G. C. Sutton, J. M. Diprose, J. Benevides, G. Thomas, Jr., J. K. H. Bamford, D. H. Bamford, and D. I. Stuart, submitted for publication). This is the first detailed X-ray analysis of a membrane-containing virus. The PRD1 capsid is stabilized by a glue protein, P30, and further by the N and C termini of the major coat proteins (51, 55; N. G. A. Abrescia, J. J. B. Cockburn, J. M. Grimes, G. C. Sutton, J. Diprose, S. J. Butcher, S. D. Fuller, San Martin, C., Burnett, R. M., D. I. Stuart, D. H. Bamford, and J. K. H. Bamford, submitted for publication). Analogous capsid stabilization has been observed in adenovirus, where several glue proteins are involved in maintaining capsid integrity (21). The PRD1 vertices are composed of the penton protein P31, the spike protein P5, and the receptor binding protein P2 (Fig. 1) (11, 23, 28, 49). The trimeric spike is attached to the pentameric penton via its N-terminal domain (11, 23), creating a symmetry mismatch as in the case of the adenovirus penton-spike complex (17, 57, 63). The symmetry mismatch is considered to be important in forming a metastable structure utilized in receptor binding, virus entry, and DNA delivery (11, 23, 43). In PRD1 the receptor binding protein P2 (66, 67) is the functional counterpart of the spike protein knob domain of adenovirus (64). The penton protein mutant ($P31^-$) lacks the spike, the receptor binding protein, and the peripentonal trimers of the coat protein, thus causing large openings at the

* Corresponding author. Mailing address: Viikki Biocenter 2, P.O. Box 56 (Viikinkaari 5), FIN-00014 University of Helsinki, Finland. Phone: 358-9-19159101. Fax: 358-9-19159098. E-mail: jaana.bamford@helsinki.fi.

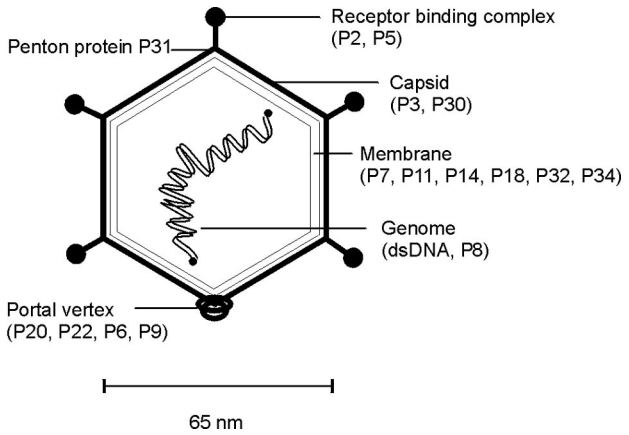

FIG. 1. Schematic presentation of PRD1 virion.

vertices (49). These openings are wide enough to allow the internal membrane to protrude as a tubular structure during DNA delivery (see below) (49). The viral membrane, which resides underneath the protein coat, closely follows the icosahedral shape of the capsid (22, 54, 55; Cockburn et al., submitted). The PRD1 membrane is approximately half lipid and half protein, as determined for the closely related phage PR4 (26). The viral lipids are selectively derived from the plasma membrane of the host cell (35, 41), and the proteins are encoded by the viral genome (10). During infection the membrane vesicle undergoes a structural transformation into a tubular tail-like structure, which has been implicated in the injection of the viral genome into the host cell (3, 29, 36). Viral proteins P7, P11, P14, P18, and P32 form the DNA delivery apparatus (29, 30). P11 has been suggested to be necessary for penetration of the bacterial outer membrane and for making the peptidoglycan layer accessible to P7, the viral transglycosylase (30, 50). Phage particles deficient in P7 protein show delayed asynchronous DNA replication and cell lysis (50). Proteins P7 and P14 are encoded by the same open reading frame (ORF), with P14 representing the C-terminal hydrophobic nonenzymatic portion of P7 (32, 50). The DNA delivery process proceeds by formation of the membrane tail tube to connect the virus interior with the host cytosol. At least viral proteins P14, P18, and P32 are involved in this process (29, 30).

One of the 12 vertices is a portal vertex with a unique protein composition of proteins P6, P9, P20, and P22 (27, 59). PRD1 genome translocation into the capsid is powered by the packaging ATPase P9, which is a structural component of the virion (38, 59), unlike packaging ATPases of most other icosahedral dsDNA bacteriophages (18). P6 is a minor protein (39), the function of which is still unknown. The small integral membrane proteins P20 and P22 are responsible for linking P6 and P9 to the viral particle and are assumed to form a packaging pore in the viral membrane (59). An intriguing question is whether the infection complex proteins P31, P5, and P2 also reside in the portal vertex.

One of the components of the PRD1 virion is the integral membrane protein P16. This protein was detected by Western blotting from the purified virus and also from cell extracts expressing the product of PRD1 ORF s cloned into a plasmid (32). On the basis of these results, ORF s was classified as gene *XVI* (12). However, the function and location of P16 have thus far been obscure, because no gene *XVI* mutants are available. In this study we isolated gene *XVI* mutants. The corresponding particles devoid of protein P16 gradually lose infectivity due to the removal of the infection vertices but not the portal vertex structure, identifying P16 as the fourth protein component of the infection vertex. This observation supports a model in which DNA is packaged into the viral particle through the portal but injected into the cell through any of the other 11 vertices. Furthermore, the absence of P16 led to a more restricted host range such that the infectivity of the mutant virus was compromised on strains with full-length lipopolysaccharide (LPS).

MATERIALS AND METHODS

Bacteria, plasmids, and phages. Bacterial strains, plasmids, and phages used in this study are listed in Table 1. Cells were grown in Luria-Bertani (LB) medium (53), and when appropriate chloramphenicol (25 μg/ml), kanamycin (25 μg/ml), and/or ampicillin (150 μg/ml) was added. For the production of wild-type, *sus408*, *sus525*, and *sus645* mutant phage particles, DS88 or HMS174(pLM2) (pALH71) cells were infected at a multiplicity of infection (MOI) of about 10. After lysis, cultures were cleared (in a Sorvall SLA3000 rotor at 7,000 rpm for 15 min at 4°C), and virus particles were concentrated from the supernatant by addition of polyethylene glycol 6000. The precipitate was collected by centrifugation (on a Sorvall SLA3000 rotor at 7,000 rpm for 20 min at 4°C), resuspended in a small volume of buffer, and purified by rate zonal centrifugation as described in reference 9. Light-scattering zones formed by viral particles were collected and harvested by differential centrifugation.

Cloning of gene *XVI*. Standard molecular cloning methods were used as described in reference 53. The region corresponding to gene *XVI* was amplified by PCR using the PRD1 genome as a template and specific primers hybridizing to the ends of the gene (nucleotide coordinates 11836 to 12189 in the PRD1 genome [GenBank accession number M69077]). The DNA fragment obtained was cloned into the pDS12 expression vector, resulting in plasmid pMV8 (Table 1).

Phage adsorption assay. Freshly made phage stocks were used in the adsorption assay. Bacteria were grown in LB medium to the optimal adsorption phase (2×10^9 CFU/ml) (34). Host cells (in 100 μl) were mixed with approximately 300 phage particles, and the mixture was incubated at 22°C for 1, 5, 10, 15, or 20 min. Cells were collected by centrifugation (in an Eppendorf microcentrifuge at 5,000 rpm for 3 min at 22°C), and the number of free (nonadsorbed) phage particles was determined by plating the supernatant on *Escherichia coli* K-12 HMS174 (pLM2).

Electron microscopy. For thin-section electron microscopy, *Salmonella enterica* serovar Typhimurium DS88 was grown to a density of 10^9 CFU/ml and infected with freshly made *sus408*, *sus645*, or wild-type phage stock at an MOI of 50. Samples were taken 7, 45, 49, or 90 min postinfection and were fixed with 3% (vol/vol) glutaraldehyde in 20 mM potassium phosphate buffer (pH 7.2). After 20 min of incubation at room temperature, cells were collected, washed twice, and prepared for transmission electron microscopy as described previously (2). For negative staining, purified virus specimens on carbon-coated grids were stained with 1% (wt/vol) ammonium molybdate (pH 6.5). Micrographs were taken with a JEOL 1200 EX electron microscope (at the Electron Microscopy unit, Institute of Biotechnology, University of Helsinki) operating at 60 kV.

Analytical methods. Sodium dodecyl sulfate-polyacrylamide gel electrophoresis was performed as described in reference 45. Western blotting was done by transferring the proteins from the gels onto polyvinylidene difluoride membranes (Millipore). Polyclonal antisera against PRD1 proteins P2 (28), P5 (32), P9 and P22 (59), and P31 (49), together with monoclonal antibodies 6T58 (anti-P6) and 7N41 (anti-P7/P14) (32), 11A401 (anti-P11) (27), and 16A201 (anti-P16) (32), were used as primary antibodies. Western blots were developed with the ECL detection system (Amersham) by using horseradish peroxidase-conjugated swine anti-rabbit immunoglobulin G (Dako) or peroxidase-conjugated horse anti-mouse immunoglobulin G (Vector) as the secondary antibody. Protein concentrations were determined with Coomassie brilliant blue by using bovine serum albumin as a standard (19).

RESULTS

Isolation and identification of phages with a defect in gene *XVI*. Wild-type PRD1 was mutagenized with *N*-methyl-*N*′-ni-

TABLE 1. Bacterial strains, phages, and plasmids used in this study

Bacterial strain, phage, or plasmid	Genotype or description[a]	Reference or source
Bacterial strains		
Salmonella enterica serovar Typhimurium LT2		
DS88	SL5676 ΔH2 H1-I::Tn*10* (Tc) (pLM2); nonsuppressor host	8
DB7154(pLM2)	DB7100 *leuA414*(Am) *hisC527*(Am) *supD10*; suppressor host for *sus408* and *sus645*	65
SH9013(pLM2)	Ra; shortened LPS	P. H. Mäkelä, National Public Health Institute, Helsinki, Finland
SL733(pLM2)	Rb_1; shortened LPS	P. H. Mäkelä, National Public Health Institute, Helsinki, Finland
SH9156(pLM2)	Rb_3; shortened LPS	P. H. Mäkelä, National Public Health Institute, Helsinki, Finland
SL761(pLM2)	Rc; shortened LPS	P. H Mäkelä, National Public Health Institute, Helsinki, Finland
Pseudomonas aeruginosa PAO (pLM2)	Full-length LPS	37
Escherichia coli K-12 HMS174	Shortened LPS	24
Phages		
PRD1	Wild type	46
sus408	Amber mutation in gene *XVI*	This study
sus525	Amber mutation in gene *XXXI*	49
sus645	Amber mutation in gene *XVI*	This study
Plasmids		
pLM2	Encodes PRD1 receptor; IncPα replicon; Km^r	37
pJB15	Encodes PRD1 receptor; IncPα replicon; Tc^r	32
pSU18	Low-copy-number cloning vector; p15A replicon; Cm^r	13
pALH71	pSU18 + PRD1 gene *VII* (12189–12986)	50
pDMI	Plasmid containing *lac* repressor; p15A replicon; Km^r	25
pDS12	Expression vector; ColE1 replicon; Ap^r	20
pMV8	pDS12 + PRD1 gene *XVI* (11836–12189)	This study

[a] Numbers refer to the PRD1 genome sequence (EMBL GenBank accession number M69077). Cm, chloramphenicol; Km, kanamycin; Ap, ampicillin; Tc, tetracycline; r, resistant.

tro-*N*-nitrosoguanidine as described previously (39). To recover nonsense mutant phages, the mutagenized viruses were plated on *S. enterica* hosts expressing tRNA suppressors for amber mutations. The resulting plaques were picked on the lawns of the corresponding suppressor and the wild-type strain DS88 to test for a lack of growth on the wild-type strain. Several amber mutant phage lines were obtained, and the plaques were further purified by two subsequent single plaque isolations on the suppressor strain. The phage mutants were screened for defects in gene *XVI* by an assay in which the defect in the phage is complemented by overexpressing the corresponding wild-type gene from a plasmid vector during mutant phage infection (10, 40). This assay is routinely performed on *E. coli* K-12 strains. However, this procedure failed because the negative control lacking the plasmid vector produced a titer of the same order of magnitude as the *S. enterica* suppressor strain (Table 2) (see below).

The amber mutant phage lines were further analyzed by infecting DS88 cells at an MOI of 10, collecting the cells before lysis, separating the cellular proteins by sodium dodecyl sulfate-polyacrylamide gel electrophoresis, and analyzing the protein content by Western blotting using a P16-specific antibody. This analysis revealed that two independent mutant isolates, *sus408* and *sus645*, did not produce protein P16 (Fig. 2). The infected-cell samples were also analyzed by Western blotting with all available PRD1-specific antibodies, showing that all of the corresponding proteins were synthesized during the mutant phage infections (data not shown) (see discussion of polar effects below). To determine whether gene *XVI* was the only one affected, the complementation assay with *sus408* and *sus645* (which failed with *E. coli* K-12 [see above]) was repeated with *S. enterica* DS88. For this assay, the wild-type gene *XVI* was cloned into the pDS12 vector under the control of the T5/*lac* hybrid promoter, yielding plasmid pMV8 (Table 1). Plasmid pDS12, together with pDMI-1 (carrying the *lac* repressor), was introduced into DS88 cells by electroporation.

TABLE 2. Complementation analysis of P16-deficient mutants and the cloned wild-type *XVI* gene

Host strain	Titer of mutant phage	
	sus408	*sus645*
Salmonella enterica serovar Typhimurium LT2		
DS88	1.6×10^7	7.7×10^6
DB7154(pLM2)	4.5×10^{11}	2.2×10^{12}
DS88(pDMI-1)(pMV8)	2.5×10^{10}	2.9×10^{10}
Escherichia coli K-12		
HMS174(pJB15)	3.4×10^{11}	1.7×10^{11}
HMS174(pJB15)(pDMI-1)(pMV8)	3.8×10^{11}	1.2×10^{11}

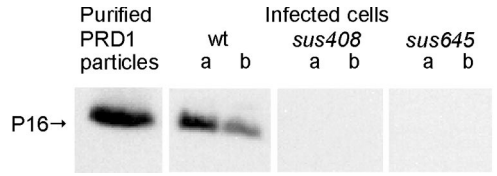

FIG. 2. Western blot of cells infected with wild-type (wt) or mutant (*sus408* or *sus645*) virus using monoclonal antibody 16A201, recognizing protein P16. Twenty-five (lanes a) or 12.5 (lanes b) μl of a 10-fold-concentrated infected-cell suspension was applied to the gel. Purified wild-type virus particles (10 μg) were used as a positive control.

Expression of protein P16 was induced with 0.2 mM isopropyl-β-thiogalactoside (IPTG). Titers of the mutant phages on DS88(pMV8)(pDMI-1) were similar to those on the suppressor strain DB7154(pLM2), revealing that the mutation in *sus408* and *sus645* was complemented by gene *XVI* (Table 2).

The location of the mutation in *sus408* and *sus645* was confirmed by DNA sequencing. In both mutants there was a change from G to A at position 11939 in the PRD1 genome, resulting in an amber (TAG) codon within gene *XVI*. Due to the mutation, gene *XVI* expresses a 34-residue N-terminal fragment of protein P16, whereas the wild-type protein has 117 residues. The two independent isolates were further used in the analyses to show that the phenotype was not affected by any other mutation induced by the mutagen.

P16-deficient phages cannot infect wild-type *S. enterica* strains. Since *sus408* and *sus645* virus stocks were able to infect *E. coli* K-12 but not *S. enterica* strain DS88 (expressing full-length LPS), the abilities of these mutant phages to infect different *S. enterica* LPS derivative strains were tested. Efficiencies of plating (EOP) were determined on DS88 and on the strains expressing a shortened LPS chain: SH9013 (Ra), SL733 (Rb_1), SH9156 (Rb_3), and SL761 (Rc) (for LPS structure and abbreviations, see reference 44). The titers showed that, although neither of the P16-deficient phages was capable of infecting DS88, they were both able to infect all the other *S. enterica* strains that had a shortened LPS chain (Table 3). The longest LPS structure among the derivative strains is that in SH9013, which lacks the outermost sugar component, the O polysaccharide. The EOP on the *E. coli* K-12 strain, which also does not express the O antigen, was comparable to the EOP on the *S. enterica* suppressor strain (Table 3), but the plaque size was smaller. Like that on DS88, the EOP on *Pseudomonas aeruginosa* PAO (expressing full-length LPS) was low. This indicates that the presence of P16 is somehow linked to the penetration of the outermost sugar component on the host cell surface.

TABLE 3. EOP of *sus408* and *sus645* on hosts expressing different LPS phenotypes

Host strain	LPS phenotype[a]	Titer of mutant phage	
		sus408	*sus645*
S. enterica			
DS88	Full length	2.6×10^5	1.1×10^6
DB7154(pLM2); suppressor	Full length	5.0×10^{11}	6.4×10^{11}
SH9013(pLM2)	Ra	4.3×10^{10}	1.6×10^{11}
SL733(pLM2)	Rb_1	3.1×10^{10}	1.7×10^{11}
SH9156(pLM2)	Rb_3	6.1×10^{10}	4.2×10^{11}
SL761(pLM2)	Rc	4.2×10^{10}	1.8×10^{11}
P. aeruginosa PAO(pLM2)	Full length	3.3×10^6	1.4×10^6
E. coli HMS174(pLM2)	Lacks O antigen	1.8×10^{11}	3.5×10^{11}

[a] For LPS structure and abbreviations, see reference 44.

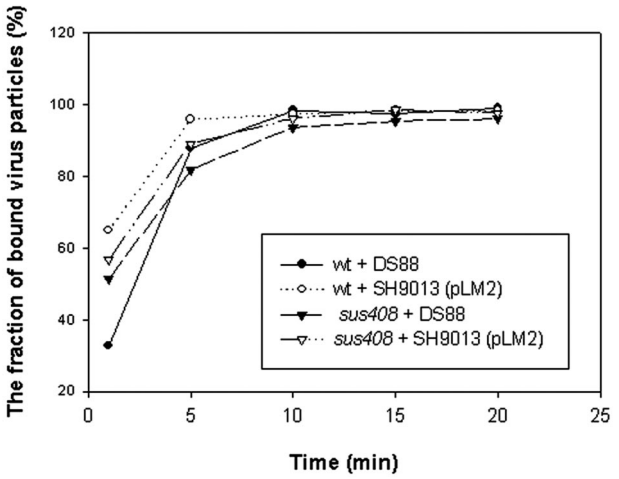

FIG. 3. Binding of wild-type (wt) and *sus408* particles to DS88 or SH9013(pLM2) cells, expressing full-length or shortened (without the O antigen) LPS, respectively.

Lack of P16 does not interfere with binding of the virus to its receptor. Since the $P16^-$ mutants were not able to infect *S. enterica* with full-length LPS, and since the plaque sizes on *E. coli* were smaller than those of the wild-type virus (data not shown), binding to the host cell receptor was determined. The binding efficiency of the P16-deficient virus was comparable to that of the wild-type virus (data for *sus408* are shown in Fig. 3). This result indicates that P16 does not interfere with the initial step of infection, which is recognition of the receptor by protein P2 (28, 30).

The mutation in gene *XVI* is polar, affecting the expression of downstream genes. Sus408 and Sus645 particles were produced in DS88 as described in Materials and Methods. Western blot analysis of the purified mutant phage particles revealed that the amounts of proteins P7 and P14 were smaller than those in PRD1 wild-type particles (data not shown). Gene *VII*/*XIV*, coding for P7 and P14, is located immediately downstream of gene *XVI* (10, 12). We tested whether the decreased amounts of P7 and P14 in the $P16^-$ mutants were due to poor expression caused by the polarity of the amber mutation in gene *XVI*. The mutant phages were grown on *E. coli* K-12 HMS174(pLM2)(pALH71), which has no tRNA suppressor activity but overexpresses proteins P7 and P14 (50). After purification of mutant particles, Western blot analysis revealed that the levels of P7 and P14 were comparable to those in wild-type particles (data not shown), indicating that the amber mutation in gene *XVI* (at position 11939) has a polar effect on downstream genes. In addition to *S. enterica* DS88, $P16^-$ particles were also produced in the *E. coli* strain overexpressing proteins P7 and P14, so as to obtain particles with only P16 altered.

P16-deficient particles lose DNA and vertex proteins upon purification. Sus408 and Sus645 particles were produced in either DS88 or HMS174(pLM2)(pALH71) cells and collected

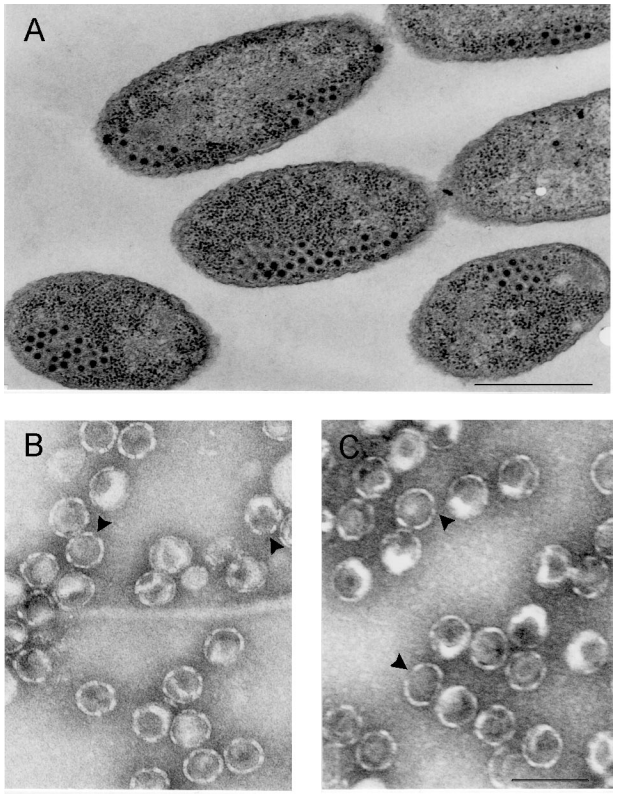

FIG. 4. (A) Electron micrograph of thin-sectioned DS88 cells infected with the *sus645* mutant and harvested 90 min postinfection. Clusters of newly assembled and packaged viruses are seen in the cell interior. Bar, 500 nm. (B) Negative-staining electron micrograph of purified *sus645* particles. (C) Control *sus525* particles, where the spike complex and the peripentonal trimers are absent (49). Arrowheads indicate positions of missing vertices. Bar, 100 nm.

by polyethylene glycol precipitation followed by purification in sucrose gradients by rate zonal centrifugation. Only one light-scattering zone corresponding to the position of empty particles without DNA was observed, whereas wild-type PRD1 infection leads to about 80% packaged and 20% empty particles (9). Thin-section electron microscopy of the infected cells showed that the particle assembly and packaging efficiency of the mutants were not altered (Fig. 4A). However, negative-staining electron microscopy of the purified P16$^-$ particles showed that they lacked DNA, and there appeared to be openings at the capsid vertices (Fig. 4B). The morphology of these particles was compared to that of Sus525 (amber mutation in gene *XXXI*) particles, which lack the vertex proteins P31, P5, and P2, as well as the peripentonal coat protein trimers and DNA (Fig. 4C) (49). The appearances of particles produced by gene *XVI* and gene *XXXI* amber mutants were similar (Fig. 4B and C). This demonstrates that the amber mutation in gene *XVI* leads, upon purification, to particles devoid of DNA and most probably of proteins P31, P5, and P2, in addition to P16 and the peripentonal trimers (see also below).

P16 stabilizes the infection vertex complex. To reveal whether the vertex complex proteins (P31, P5, and P2) were present in purified P16$^-$ mutant particles, we analyzed the particles by Western blotting. As shown in Fig. 5A, the amounts of all three vertex complex proteins were drastically smaller in the mutants

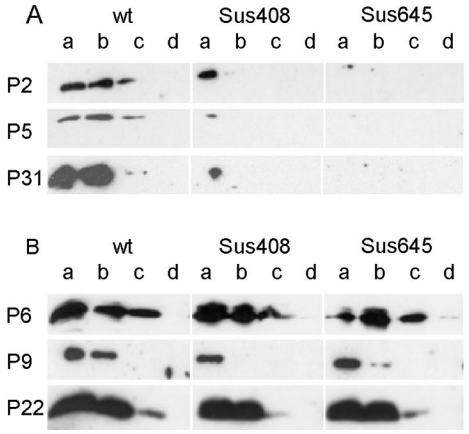

FIG. 5. Western blot of purified wild-type (wt) and P16$^-$ mutant (*sus408* or *sus645*) PRD1 particles. Lanes contain 10 (a), 5 (b), 1 (c), or 0.2 (d) μg of virus. (A) Detection with antibodies against the vertex complex proteins P2, P5, and P31. (B.)Detection with antibodies against the packaging vertex proteins P6, P9, and P22.

than in the wild-type virus. In a similar assay, the portal vertex proteins P6 and P22 were detected at levels comparable to those in wild-type particles (Fig. 5B). This demonstrates that when P16 is missing, the receptor binding spike complex is dissociated from the virus upon particle purification but the portal structure involved in DNA packaging is not. It should be noted that the amount of the packaging ATPase P9 seems to be slightly smaller in P16$^-$ particles than in wild-type PRD1 (Fig. 5B). This was not due to changes in protein P9, since the gene sequence was determined to be wild type. To confirm that the absence of the vertex proteins was linked to the absence of P16 and not to changes in penton protein P31 (known to lead to the absence of the vertex proteins), the gene *XXXI* sequence was also determined for the *sus408* and *sus645* mutants. No changes were observed, suggesting that the lack of P16 is sufficient to cause the vertex dissociation. To test the stability of the P16-deficient mutant, the phage stock was stored at 4°C and its infectivity was assayed on the wild-type *E. coli* strain.

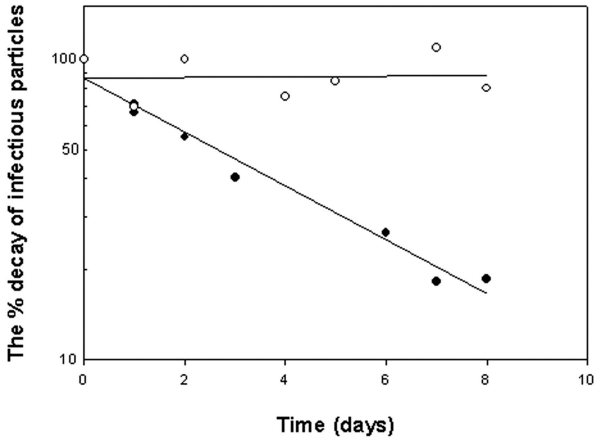

FIG. 6. Decay of wild-type (open circles) and *sus408* (filled circles) infectivity. Virus stocks were grown in HMS174(pLM2)(pALH71) in LB medium. Phage stocks were stored at 4°C, and infectivity was determined periodically.

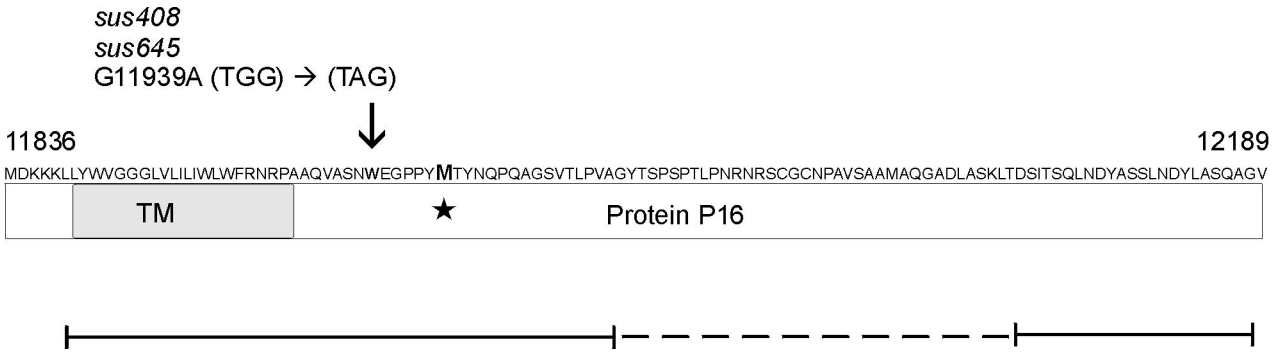

FIG. 7. Schematic representation of protein P16, showing the position of the *sus408* and *sus645* amber mutations in tryptophan 35 (arrow). Star indicates the methionine residue, which was resolved in the electron density map of the seleno-methionine-labeled virus crystal (Cockburn et al., submitted). Solid line, residues visible in the electron density map; dashed line, residues that were disordered (or not isosahedrally ordered). The resolved transmembrane helix (TM) is shaded.

The infectivity of the P16-deficient mutant decreased much more rapidly than that of the wild-type virus stock (Fig. 6). This is consistent with the finding that P16$^-$ particles spontaneously lose the infection vertex structure.

DISCUSSION

The usage of *E. coli* K-12 cells in the complementation assay prevented detection of the P16$^-$ phenotype among the amber mutants due to the nonessential nature of protein P16. However, P16 was essential for infecting *S. enterica* and *P. aeruginosa* cells. When different *Salmonella* strains were tested, the gene *XVI* mutant particles were unable to infect DS88 with the full-length LPS but were able to infect cells without the outermost sugar component, the O antigen. The absence of P16 does not affect the recognition of the host cell, since P16-deficient mutants were able to bind to DS88 cells with the same efficiency as wild-type PRD1. The nature of this phenomenon is obscure at the moment, but it might reflect the instability of the vertex structure in the P16-deficient mutant upon binding to O-antigen-containing cells.

The absence of protein P16 did not affect DNA packaging or virion assembly. However, the mutant phages lost their infectivity much more rapidly upon storage than the wild-type phage (Fig. 6). When P16$^-$ mutant phages were purified, the infection vertex proteins P2, P5, and P31, as well as DNA and most probably the peripentonal coat protein trimers, were released (Fig. 4 and 5). This result identifies P16 as the fourth protein of the infection vertex complex, with the function of increasing the vertex stability.

Protein P16 has a predicted transmembrane region in its N terminus and a methionine residue ~16 amino acids downstream of this region. These signature elements allowed identification of this region as the N terminus of P16 underneath the peripentonal coat protein trimers around the icosahedral fivefold axis in the electron density map of the crystallized virion (Fig. 7). Residues 7 to 56 and 94 to 116 were visible in the map. The observed methionine was ~11 residues above the membrane surface, and the N terminus of P16 is embedded in the membrane as a transmembrane helix. The N and C termini have extensive interactions with the peripentonal trimers, whereas the disordered portion of P16 resides underneath the vertex (Cockburn et al., submitted). These results explain the stabilizing effect of P16 on the vertex structure. We were unable to determine whether the 34-residue N-terminal amber fragment of P16 was assembled into the virus, since none of the available monoclonal antibodies against P16 recognizes this fragment. The function of P16 might be analogous to that of one of the adenovirus cementing proteins, polypeptide VI, which secures the ring of peripentonal hexons and connects the capsid to the viral core (21, 58).

The properties of the P16-deficient mutants and the location of the protein in the particle suggest that P16 anchors the vertex structure to the viral membrane. An interesting finding is that the release of the infection vertex proteins from the particle has no effect on the presence of the portal vertex proteins P6 and P22. The decreased amount of the packaging ATPase P9 in particles produced by gene *XVI* mutants could be explained by assuming that DNA release destabilizes this protein, which is brought to the particle by the packaging reaction (N. J. Strömsten, and J. K. H. Bamford, unpublished data). Based on these results, it is most probable that the single portal vertex does not contain the spike complex proteins composing the infection vertices. This supports a model where DNA is packaged into the virus particle via the unique portal vertex and ejected through any of the remaining 11 vertices.

This work reveals that the infection vertex is more complex than previously predicted. The receptor binding vertex, composed of the penton, the spike, and the receptor binding protein, is linked to the viral membrane by protein P16. There must exist a signaling pathway that triggers entry-associated events upon binding of the receptor. The signal is transmitted via the trimeric spike protein symmetry mismatch to the penton protein and, further, to the membrane protein P16, resulting in DNA exit from the membrane vesicle aided by proteins P7/P14, P11, P18, and P32.

ACKNOWLEDGMENTS

This study was supported by research grants 1201964 (to J.K.H.B.), 1202855, and 1202108 (to D.H.B.) from the Academy of Finland (Finnish Center of Excellence Program [2000-2005]).

We thank Marika Vitikainen for providing plasmid pMV8. The technical assistance of Sara Ollila and Anna Rantala is gratefully acknowledged.

REFERENCES

1. **Ackermann, H.-W., R. Roy, M. Martin, M. R. V. Murthy, and W. A. Smirnoff.** 1978. Partial characterization of a cubic *Bacillus* phage. Can. J. Microbiol. **24:**986–993.
2. **Bamford, D. H., and L. M. Mindich.** 1980. Electron microscopy of cells infected with nonsense mutants of bacteriophage ϕ6. Virology **71:**222–228.
3. **Bamford, D. H., and L. M. Mindich.** 1982. Structure of the lipid-containing bacteriophage PRD1: disruption of wild-type and nonsense mutant phage particles with guanidine hydrochloride. J. Virol. **44:**1031–1038.
4. **Bamford, D. H., J. Caldentey, and J. K. H. Bamford.** 1995. Bacteriophage PRD1: a broad host range dsDNA tectivirus with an internal membrane. Adv. Virus Res. **45:**281–319.
5. **Bamford, D. H., and H.-W. Ackermann.** 2000. Family *Tectiviridae*, p. 111–116. *In* M. H. V. van Regenmortel, C. M. Fauquet, D. H. L. Bishop, E. B. Carstens, M. K. Estes, S. M. Lemon, J. Maniloff, M. A. Mayo, D. J. McGeoch, C. R. Pringle, and R. B. Wickner (ed.), Virus taxonomy: classification and nomenclature of viruses. Seventh report of the International Committee on Taxonomy of Viruses. Academic Press, San Diego, Calif.
6. **Bamford, D. H., R. M. Burnett, and D. I. Stuart.** 2002. Evolution of viral structure. Theor. Popul. Biol. **61:**461–470.
7. **Bamford, D. H.** 2003. Do viruses form lineages across different domains of life? Res. Microbiol. **154:**231–236.
8. **Bamford, J. K. H., and D. H. Bamford.** 1990. Capsomer proteins of bacteriophage PRD1, a bacterial virus with a membrane. Virology **177:**445–451.
9. **Bamford, J. K. H., and D. H. Bamford.** 1991. Large scale purification of membrane-containing bacteriophage PRD1 and its subviral particles. Virology **181:**348–352.
10. **Bamford, J. K. H., A.-L. Hänninen, T. M. Pakula, P. M. Ojala, N. Kalkkinen, M. Frilander, and D. H. Bamford.** 1991. Genome organization of PRD1, a membrane-containing bacteriophage infecting *E. coli.* Virology **183:**658–676.
11. **Bamford, J. K. H., and D. H. Bamford.** 2000. A new mutant class, made by targeted mutagenesis, of phage PRD1 reveals that protein P5 connects the receptor binding protein to the vertex. J. Virol. **74:**7781–7786.
12. **Bamford, J. K. H., J. Cockburn, J. Diprose, J. M. Grimes, G. Sutton, D. I. Stuart, and D. H. Bamford.** 2002. Diffraction quality crystals of PRD1, a 66 MDa dsDNA virus with an internal membrane. J. Struct. Biol. **139:**103–112.
13. **Bartolomé, B., Y. Jubete, E. Martínez, and F. Cruz.** 1991. Construction and properties of a family of pACYC184-derived cloning vectors compatible with pBR322 and its derivatives. Gene **102:**75–78.
14. **Belnap, D. M., and A. C. Steven.** 2000. 'Déjà vu all over again': the similar structures of bacteriophage PRD1 and adenovirus. Trends Microbiol. **8:**91–93.
15. **Benson, S. D., J. K. H. Bamford, D. H. Bamford, and R. M. Burnett.** 1999. Viral evolution revealed by bacteriophage PRD1 and human adenovirus coat protein structures. Cell **98:**825–833.
16. **Benson, S. D., J. K. H. Bamford, D. H. Bamford, and R. M. Burnett.** 2002. The X-ray crystal structure of P3, the major coat protein of the lipid-containing bacteriophage PRD1, at 1.65 Å resolution. Acta Crystallogr. Sect. D **58:**39–59.
17. **Bewley, M. C., K. Springer, Y. B. Zhang, P. Freimuth, and J. M. Flanagan.** 1999. Structural analysis of the mechanism of adenovirus binding to its human cellular receptor, CAR. Science **286:**1579–1583.
18. **Black, L. W.** 1989. DNA packaging in dsDNA bacteriophages. Annu. Rev. Microbiol. **43:**267–292.
19. **Bradford, M. M.** 1976. A rapid and sensitive method for the quantitation of microgram quantities of protein utilizing the principle of protein-dye binding. Anal. Biochem. **72:**248–254.
20. **Bujard, H., R. Gentz, M. Lanzer, D. Stueber, M. Mueller, I. Ibrahimi, M.-T. Haeuptle, and B. Dobberstein.** 1987. A T5 promoter-based transcription-translation system for the analysis of proteins *in vitro* and *in vivo*. Methods Enzymol. **155:**416–433.
21. **Burnett, R. M.** 1997. The structure of adenovirus, p. 209–238. *In* W. Chiu, R. M. Burnett, and R. L. Garcea (ed.), Structural biology of viruses. Oxford University Press, New York, N.Y.
22. **Butcher, S. J., D. H. Bamford, and S. D. Fuller.** 1995. DNA packaging orders the membrane of bacteriophage PRD1. EMBO J. **14:**6078–6086.
23. **Caldentey, J., R. Tuma, and D. H. Bamford.** 2000. Assembly of bacteriophage PRD1 spike complex: the role of the multidomain protein P5. Biochemistry **39:**10566–10573.
24. **Campbell, J. L., C. C. Richardson, and F. W. Studier.** 1978. Genetic recombination and complementation between bacteriophage T7 and cloned fragments of T7 DNA. Proc. Natl. Acad. Sci. USA **75:**2276–2280.
25. **Certa, U., W. Bannwarth, D. Stüber, R. Gentz, M. Lanzer, S. Le Grice, F. Guillot, I. Wendler, G. Hunsmann, H. Bujard, and J. Mous.** 1986. Subregions of a conserved party of the HIV gp41 transmembrane protein are differentially recognized by antibodies of infected individuals. EMBO J. **5:**3051–3056.
26. **Davis, T. N., E. D. Muller, and J. E. Cronan.** 1982. The virion of the lipid-containing bacteriophage PR4. Virology **120:**287–306.
27. **Gowen, B., J. K. H. Bamford, D. H. Bamford, and S. D. Fuller.** 2003. The tailless icosahedral membrane virus PRD1 localizes the proteins involved in genome packaging and injection at a unique vertex. J. Virol. **77:**7863–7871.
28. **Grahn, A. M., J. Caldentey, J. K. H. Bamford, and D. H. Bamford.** 1999. Stable packaging of phage PRD1 DNA requires adsorption protein P2, which binds to the IncP plasmid-encoded conjugative transfer complex. J. Bacteriol. **181:**6689–6696.
29. **Grahn, A. M., R. Daugelavicius, and D. H. Bamford.** 2002. The small viral membrane-associated protein P32 is involved in bacteriophage PRD1 DNA entry. J. Virol. **76:**4866–4872.
30. **Grahn, A. M., R. Daugelavicius, and D. H. Bamford.** 2002. Sequential model of phage PRD1 DNA delivery; active involvement of the viral membrane. Mol. Microbiol. **46:**1199–1209.
31. **Grahn, A. M., S. J. Butcher, J. K. H. Bamford, and D. H. Bamford.** PRD1—dissecting the genome, structure and entry. *In* R. Calendar (ed.), The bacteriophages, 2nd ed., in press. Oxford University Press, New York, N.Y.
32. **Hänninen, A.-L., D. H. Bamford, and J. K. H. Bamford.** 1997. Probing phage PRD1-specific proteins with monoclonal and polyclonal antibodies. Virology **227:**198–206.
33. **Harrison, S. C., A. J. Olson, C. E. Schutt, F. K. Winkler, and G. Bricogne.** 1978. Tomato bushy stunt virus at 2.9 Å resolution. Nature **276:**368–373.
34. **Kotilainen, M. M., A. M. Grahn, J. K. H. Bamford, and D. H. Bamford.** 1993. Binding of an *Escherichia coli* double-stranded DNA virus PRD1 to a receptor coded by an IncP-type plasmid. J. Bacteriol. **175:**3089–3095.
35. **Laurinavičius, S., R. Käkelä, P. Somerharju, and D. H. Bamford.** 2004. Phospholipid molecular species profiles of tectiviruses infecting Gram-negative and Gram-positive hosts. Virology **322:**328–336.
36. **Lundström, K. H., D. H. Bamford, E. T. Palva, and K. Lounatmaa.** 1979. Lipid-containing bacteriophage PR4: structure and life cycle. J. Gen. Virol. **43:**538–592.
37. **Mindich, L., J. Cohen, and M. Weisburd.** 1976. Isolation of nonsense suppressor mutants in *Pseudomonas*. J. Bacteriol. **126:**177–182.
38. **Mindich, L., D. Bamford, C. Goldthwaite, M. Laverty, and G. MacKenzie.** 1982. Isolation of nonsense mutants of lipid-containing bacteriophage PRD1. J. Virol. **44:**1013–1020.
39. **Mindich, L., D. Bamford, T. McGraw, and G. MacKenzie.** 1982. Assembly of bacteriophage PRD1: particle formation with wild-type and mutant viruses. J. Virol. **44:**1021–1030.
40. **Mindich, L., and T. McGraw.** 1983. Molecular cloning of bacteriophage PRD1 genomic fragments. Mol. Gen. Genet. **190:**233–236.
41. **Myung, H., and J. E. Cronan, Jr.** 1994. Lipid selection in the assembly of the phospholipid bilayer membrane of the lipid-containing bacteriophage PR4. Virology **198:**17–24.
42. **Nandhagopal, N., A. A. Simpson, J. R. Gurnon, X. Yan, T. S. Baker, M. V. Graves, J. L. Van Etten, and M. G. Rossmann.** 2002. The structure and evolution of the major capsid protein of a large, lipid-containing DNA virus. Proc. Natl. Acad. Sci. USA **99:**14758–14763.
43. **Nemerow, G. R., and P. L. Stewart.** 1999. Role of α_v integrins in adenovirus cell entry and gene delivery. Microbiol. Mol. Biol. Rev. **63:**725–734.
44. **Nikaido, H., and M. Vaara.** 1987. Outer membrane, p. 7–22. *In* F. C. Neidhardt, J. L. Ingraham, K. B. Low, B. Magasanik, M. Schaechter, and H. E. Umbarger (ed.), *Escherichia coli* and *Salmonella typhimurium*: cellular and molecular biology. American Society for Microbiology, Washington, D.C.
45. **Olkkonen, V. M., and D. H. Bamford.** 1989. Quantitation of the adsorption and penetration stages of bacteriophage ϕ6 infection. Virology **171:**229–238.
46. **Olsen, R. H. M., J.-S. Siak, and R. H. Gray.** 1974. Characteristics of PRD1, a plasmid-dependent broad host range DNA bacteriophage. J. Virol. **14:**689–699.
47. **Ravantti, J. J., A. Gaidelyte, D. H. Bamford, and J. K. H. Bamford.** 2003. Comparative analysis of the genomes of bacterial viruses Bam35, infecting a gram-positive host, and PRD1, infecting gram-negative hosts, demonstrates a viral lineage. Virology **313:**401–414.
48. **Rossmann, M. G., E. Arnold, J. W. Erickson, E. A. Frankenberger, J. P. Griffith, H. J. Hecht, J. E. Johnson, G. Kamer, M. Luo, A. G. Mosser, R. R. Rueckert, B. Sherry, and G. Vriend.** 1985. Structure of a human common cold virus and functional relationship to other picornaviruses. Nature **317:**145–153.
49. **Rydman, P. S., J. Caldentey, S. J. Butcher, S. D. Fuller, T. Rutten, and D. H. Bamford.** 1999. Bacteriophage PRD1 contains a labile receptor-binding structure at each vertex. J. Mol. Biol. **291:**575–587.
50. **Rydman, P. S., and D. H. Bamford.** 2000. Bacteriophage PRD1 DNA entry uses a viral membrane-associated transglycosylase activity. Mol. Microbiol. **37:**356–363.
51. **Rydman, P. S., J. K. H. Bamford, and D. H. Bamford.** 2001. A minor capsid protein P30 is essential for bacteriophage PRD1 capsid assembly. J. Mol. Biol. **313:**785–795.
52. **Salas, M.** 1991. Protein-priming of DNA replication. Annu. Rev. Biochem. **60:**39–71.
53. **Sambrook, J., and D. W. Russell.** 2001. Molecular cloning: a laboratory manual, 3rd ed. Cold Spring Harbor Laboratory Press, Cold Spring Harbor, N.Y.
54. **San Martín, C., R. M. Burnett, F. Haas, R. Heinkel, T. Rutten, S. D. Fuller, S. J. Butcher, and D. H. Bamford.** 2001. Combined EM/X-ray imaging yields

a quasi-atomic model of the adenovirus-related bacteriophage PRD1 and shows key capsid and membrane interactions. Structure **9:**917–930.

55. **San Martín, C., J. T. Huiskonen, J. K. H. Bamford, S. J. Butcher, S. D. Fuller, D. H. Bamford, and R. M. Burnett.** 2002. Minor proteins, mobile arms and membrane-capsid interactions in bacteriophage PRD1 assembly. Nat. Struct. Biol. **9:**756–763.
56. **Skrdla, M. P., D. E. Burbank, Y. Xia, R. H. Meints, and J. L. Van Etten.** 1984. Structural proteins and lipids in a virus, PBCV-1, which replicates in a *Chlorella*-like alga. Virology **135:**308–315.
57. **Stewart, P. L., R. M. Burnett, M. Cyrklaff, and S. D. Fuller.** 1991. Image reconstruction reveals the complex molecular organization of adenovirus. Cell **67:**145–154.
58. **Stewart, P. L., S. D. Fuller, and R. M. Burnett.** 1993. Difference imaging of adenovirus: bridging the resolution gap between X-ray crystallography and electron microscopy. EMBO J. **12:**2589–2599.
59. **Strömsten, N. J., D. H. Bamford, and J. K. H. Bamford.** 2003. The unique vertex of bacterial virus PRD1 is connected to the viral internal membrane. J. Virol. **77:**6314–6321.
60. **Van Etten, J. L., L. Lane, and R. Meints.** 1991. Viruses and virus-like particles of eukaryotic algae. Microbiol. Rev. **55:**586–620.
61. **Van Etten, J. L., and R. H. Meints.** 1999. Giant viruses infecting algae. Annu. Rev. Microbiol. **53:**447–494.
62. **Van Etten, J. L., M. V. Graves, D. G. Müller, W. Boland, and N. Delaroque.** 2002. *Phycodnaviridae*—large DNA algal viruses. Arch. Virol. **147:**1479–1516.
63. **van Oostrum, J., and R. M. Burnett.** 1985. Molecular composition of the adenovirus type 2 virion. J. Virol. **56:**439–448.
64. **van Raaij, M. J., A. Mitraki, G. Lavigne, and S. Cusack.** 1999. A triple beta-spiral in the adenovirus fibre shaft reveals a new structural motif for a fibrous protein. Nature **401:**935–938.
65. **Winston, F., D. Botstein, and J. H. Miller.** 1979. Characterization of amber and ochre suppressors in *Salmonella typhimurium*. J. Bacteriol. **137:**433–439.
66. **Xu, L., S. J. Butcher, S. D. Benson, D. H. Bamford, and R. M. Burnett.** 2000. Crystallization and preliminary X-ray analysis of receptor-binding protein P2 of bacteriophage PRD1. J. Struct. Biol. **131:**159–163.
67. **Xu, L., S. D. Benson, S. J. Butcher, D. H. Bamford, and R. M. Burnett.** 2003. The receptor-binding protein P2 of PRD1, a bacteriophage targeting antibiotic-resistant bacteria, has a novel structural fold suggesting multiple functions. Structure **11:**309–322.
68. **Yan, X., N. H. Olson, J. L. Van Etten, M. Bergoin, M. G. Rossmann, and T. S. Baker.** 2000. Structure and assembly of large lipid-containing dsDNA viruses. Nat. Struct. Biol. **7:**101–103.